Diffusion profiles of high dosage Cr and V ions implanted into silicon

P. Zhang, F. Stevie, R. Vanfleet, R. Neelakantan, M. Klimov, D. Zhou, and L. Chow
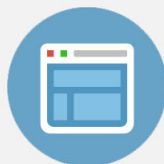
Diffusion profiles of high dosage Cr and V ions implanted into silicon

P. Zhang[a)]
Department of Physics, University of Central Florida, Orlando, Florida 32816

F. Stevie
Analytical Instrumentation Facility, North Carolina State University, Raleigh, North Carolina 27695

R. Vanfleet[b)]
Department of Physics, University of Central Florida, Orlando, Florida 32816, and Advanced Materials Processing & Analysis Center, University of Central Florida, Orlando, Florida 32816

R. Neelakantan
Department of Mechanical, Materials, and Aerospace Engineering, University of Central Florida, Orlando, Florida 32816

M. Klimov
Advanced Materials Processing & Analysis Center, University of Central Florida, Orlando, Florida 32816

D. Zhou
Advanced Materials Processing & Analysis Center, University of Central Florida, Orlando, Florida 32816, and Department of Mechanical, Materials, and Aerospace Engineering, University of Central Florida, Orlando, Florida 32816

L. Chow[c)]
Department of Physics, University of Central Florida, Orlando, Florida 32816

The depth profiles of high dosage $^{52}Cr^+$ and $^{51}V^+$ ions implanted in (100) crystalline silicon after thermal anneal at temperatures between 300 °C and 1000 °C are studied by secondary ion mass spectrometry and cross-sectional transmission electron microscopy. At dosages of 1×10^{15} ions/cm^2 and above, the surface layer of silicon substrate is amorphized. During the subsequent thermal annealing, the depth profiles of the implanted ions are strongly coupled with the solid phase epitaxial growth of amorphous silicon. Silicide precipitate formation is important to understand the differences between Cr and V diffusion. After anneal of the 1×10^{15} ions/cm^2 implanted samples at 900 °C and 1000 °C, most of the Cr has left the silicon, but only 10% of the V has escaped. The 1×10^{14} ions/cm^2 Cr-implanted sample shows Cr ions exist only near the surface after 1000 °C anneal. The V-implanted sample, on the other hand, only shows a narrowing of the V profile after 1000 °C anneal. © *2004 American Institute of Physics.*
[DOI: 10.1063/1.1756221]

I. INTRODUCTION

It is well known that transition metal impurities in silicon, even at relatively low concentration, can adversely impact the yield, reliability, and performance of semiconductor devices.[1] Thus, understanding the behavior of transition metal impurities in silicon is of paramount importance to semiconductor industries and has been the subject of intense studies over several decades.[1,2] The properties of $3d$ transition metals in silicon such as those of Fe in silicon are well understood.[3,4] However, fundamental properties such as diffusivity and solubility of Cr[5-11] and V[11-13] in silicon are still poorly studied. To summarize the current status of the Cr and V diffusion properties in silicon, we tabulate the existing

measurements of diffusion coefficient of Cr and V in silicon, D_{Cr}, D_V in Table I. It can be seen from the table that even though the diffusivity data of Cr in silicon are limited, they are reasonably consistent with each other, while in the case of vanadium, the situation is more complicated. The existing data of V diffusivity in silicon do not agree with each other and more work is needed.

Ion implantation has been and will continue to be an important technique in semiconductor device processing and manufacturing. It is well known that this energetic process will generate defects in the target substrate and, with high enough implantation dosage, an amorphous layer can form as a result of the implantation. For silicon crystal, the typical effective threshold damage density of $3d$ transition metals is approximately 7×10^{20} keV/cm^3,[14] which corresponds to an implantation dosage of roughly 10^{14} ions/cm^2. During thermal annealing after ion implantation, different defects will form with different damage dosages and/or different annealing temperatures.[14] The interactions between these defects and impurities make the diffusion process very complex. For

a)Current address: Department of Materials Science, University of California, and Materials Science Division, Lawrence Berkeley National Laboratory, Berkeley, CA 94720; electronic mail: pzhang@lbl.gov

b)Current address: Department of Physics, Brigham Young University, Provo, UT 84602; electronic mail: rrv3@byu.edu

c)Author to whom correspondence should be addressed; electronic mail: chow@ucf.edu

TABLE I. Diffusivities of chromium and vanadium in silicon, $D = D_0 \exp(-H_M/k_B T)$.

Metal	D_0 (cm²/s)	H_M (eV)	Temperature (°C)	D (cm²/s)	Ref.
Cr	1.0×10^{-2}	0.99	900–1200	$1.2 \times 10^{-6(a)}$	5, 6
Cr	6.8×10^{-4}	0.79	23–400	$8.3 \times 10^{-10(b)}$	11, 13
Cr				$1.5 \times 10^{-7(c)}$	8
Cr				$2.0 \times 10^{-17(d)}$	9
V	9×10^{-3}	1.55	600–800	$4.7 \times 10^{-10(e)}$	11, 13
V	0.61	2.8	1100–1250	$3.4 \times 10^{-11(f)}$	12

(a)At 1000 °C.
(b)At 400 °C.
(c)At 850 °C.
(d)At 25 °C.
(e)At 800 °C.
(f)At 1100 °C.

example, {311} defects cause the so-called transient enhanced diffusion of boron,[15] while dislocation loops can trap impurities such as aluminum[16] and boron.[17,18] It is almost impossible to understand the diffusion behavior without considering the evolution of defects and their interactions with impurities during annealing.

Earlier work by Wilson *et al.*[19,20] on the annealing behaviors of implanted Cr in Si have demonstrated the richness of the study of diffusion of implanted species. Wilson *et al.* carried out the ion energy dependence study of the Cr depth profile after thermal annealing. They found that at low energy ($E < 100$ keV), and 4×10^{13} ions/cm² dosage, the Cr ions migrate to the surface. For the same dosage but at higher implantation energy, the Cr ions deplete strongly at the near-surface region, while at deeper depth, the Cr ions remain immobile up to 840 °C, after a 20-min anneal. More recently, 17 elements have been implanted into silicon (100) single crystal substrates and several categories of diffusion behaviors have been reported based on secondary ion mass spectrometry (SIMS) depth profiles,[21] including those of Cr and V. However, a detailed study of the diffusion of Cr and V as a function of dosage would provide more information on the role of defects generated by ion implantation during the annealing of an implanted sample. Here, we will report the SIMS depth profiles of high-dosage implanted Cr and V ions in Si as a function of annealing temperature and implant dose. Cross-sectional transmission electron microscopy (XTEM) micrographs are combined with the SIMS data to understand the interaction between diffusion behavior and defect evolution.

II. EXPERIMENTAL PROCEDURES

^{52}Cr$^+$ and ^{51}V$^+$ ions are implanted into (100) *p*-type *B*-doped 10–20 Ω-cm CZ single-crystalline silicon substrates with dosages of 1×10^{14} and 1×10^{15} ions/cm² at room temperature. In this paper, unless it is pointed out specifically, the ion implantation energy is 200 keV. The implantation was carried out at Implant Sciences Corporation. The ion-implanted samples are then annealed at 300, 500, 700, 900, and 1000 °C, respectively, for 30 min in a high-purity argon atmosphere (99.999%).

To obtain depth profiles of Cr and V ions, SIMS characterization is carried out with a CAMECA IMS-3f at the UCF/

Agere Materials Characterization Facility, using a 150 nA O_2^+ primary beam with impact energy of 5.5 keV and an effective impact angle of 40° from normal. The focused primary beam of oxygen ions is rastered over a 200×200 μm² area, with detection of ions from an area of 60 μm diameter at the center of the raster. The sputtering rate is approximately 0.5 nm/s. The depth scale is established by measuring the crater depth with an Alphastep profilemeter, and the concentration is calibrated with the implantation dosages of the as-implanted samples.

TEM samples were prepared in cross section using one of two techniques: focused ion beam (FIB) *ex situ* lift out and tripod polishing. Analysis was carried out in an FEI Tecnai F30 TEM operating at 300 keV. Images were recorded on a CCD camera.

III. RESULTS AND DISCUSSIONS

A. Chromium implantation

Here, we will present the experimental results of Cr-implanted samples after different annealing treatments. Two different implantation dosages are used: 1.0×10^{15} ions/cm², which is enough to generate an amorphous layer, and 1.0×10^{14} ions/cm², which is below the amorphization critical dosage.

Figure 1 presents the SIMS depth profiles of Cr atoms in the as-implanted and annealed samples with an implantation dosage of 1.0×10^{15} ions/cm². In order to study the correlation between the redistribution of Cr impurities and the evolution of possible defects in silicon generated by ion implantation, the corresponding XTEM micrographs are shown with the *x* axis scaled to the same dimension as the SIMS profile.

From Fig. 1(a), we can see that this implantation dosage is high enough to generate an amorphous layer on the front surface of the Si substrate. After the 30-min 300 °C anneal [Fig. 1(b)], the Cr profile does not change significantly because the Cr diffusivity at this temperature is relatively low and solid phase epitaxial growth (SPEG) is not yet activated at this low temperature.

Annealed at 500 °C, Cr movement begins as shown in Fig. 1(c). A concentration peak is formed at a depth of 0.27 μm near the end of range (EOR) defects, and a pileup peak appears at a depth of 0.18 μm, which corresponds to the new amorphous/crystalline (a/c) interface. Between these two peaks, a sharp minimum appears at a depth of 0.23 μm. With this annealing condition, the concentration profile in the amorphous layer before the depth of 0.18 μm does not change appreciably after 500 °C annealing. As a comparison, the diffusion length $\sqrt{4Dt}$ of Cr in c-Si for 30 min at this temperature is 47 μm.[2] The SIMS depth profiles imply a much lower diffusivity of Cr in amorphous silicon than that in crystalline silicon. The lower diffusivity in amorphous silicon is observed for other metals such as Cu,[22] Pd,[23] and Ni.[24] The SPEG velocity is 0.46 Å/s at 500 °C, which is about 3–4 times faster than the intrinsic SPEG velocity.[25–27] Since the boron doping level in our sample is low, the boron-enhanced SPEG[27,28] can be ignored and thus this enhancement in our case is only a result of high Cr concentration.
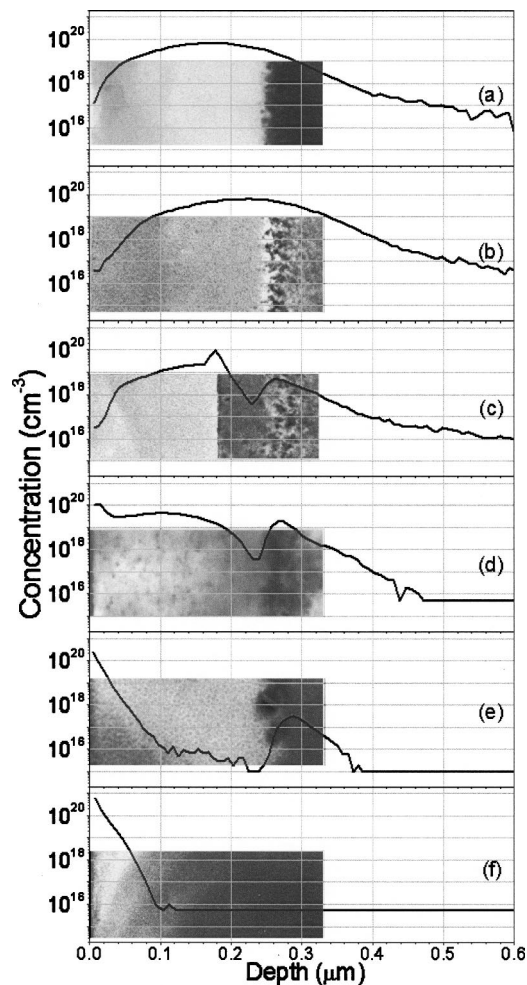
FIG. 1. SIMS depth profiles of ^{52}Cr implanted into silicon substrate at ion energy of 200 keV and a dosage of 1.0×10^{15} ions/cm^2. (a) as implanted; (b) after 300 °C anneal; (c) after 500 °C anneal; (d) after 700 °C anneal; (e) after 900 °C; and (f) after 1000 °C anneal. The background in each panel is the XTEM micrograph corresponding to the SIMS profile.

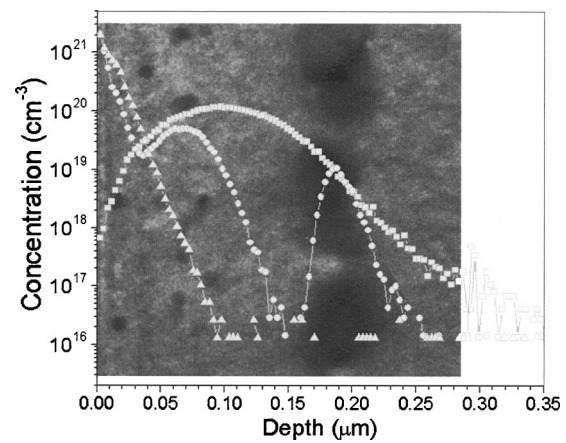FIG. 2. SIMS depth profiles of ^{52}Cr implanted into silicon substrate at ion energy of 120 keV and a dosage of 1.1×10^{15} ions/cm^2. [□ as implanted, ○ 900 °C, △ 1000 °C] The background is an XTEM micrograph of sample annealed at 900 °C.

After 700 °C annealing, the recrystallization is completed but there is anomalous diffusion behavior near and beyond the EOR defects as we can observe in Fig. 1(d). Compared with the SIMS profile in Fig. 1(c), the concentration at a depth of 0.27 µm has increased three times and the peak width is also decreased, which cannot be explained by normal diffusion. This abnormal behavior could be a result of the formation of chromium disilicide molecules, CrSi$_x$ ($x \approx 2$) precipitates or just silicon clusters trapping chromium atoms at the EOR, as it is well known that under this annealing temperature, the EOR dislocation loops generated by ion implantation will evolve into interstitial clusters,[15,29] and at the same time the formation of CrSi$_2$ is possible at a temperature as low as 450 °C.[30] However, the determination of phase is not possible without more advanced instrumentation such as nano electron diffraction, and is worth a separate study. Similar anomalous behaviors have been observed in other metal–silicon systems such as Er:Si reported by Ren *et al.*[31] The plateau-like profiles near the surface have been observed for fast diffusers such as Au,[32] Cu,[33] Ni,[34] etc. This profile might be simulated based on the model suggested by Aleksandrov *et al.*[35] if transition layer width and appropriate dependence of segregation coefficient on concentration are chosen. Campisano *et al.*[33] suggested that the impurities diffuse so fast that they cannot be trapped at the moving a/c interface; instead, they will diffuse into the amorphous silicon and get trapped by the defects intrinsic to amorphous silicon. It appears that once the Cr atoms are trapped, the complexes are immobile at 700 °C. The flat concentration profile in the newly crystallized layer might be the accommodation ability of the defects in a-Si, rather than the solubility of Cr in a-Si, because similar behavior is observed in 1.0×10^{15} ions/cm^2 vanadium-implanted samples to be shown later, where the V-trap complexes are very stable even at temperature as high as 1000 °C. From SIMS depth profiles in both Figs. 1(c) and (d), we can observe a concentration valley between a depth of 0.15 µm and the EOR defects. From the XTEM micrographs, it is clear that this area is less defective than the other areas in the micrographs. Thus, this area has lower accommodation ability for Cr impurities to form Cr–defect complexes. It should be mentioned again that once the impurities are trapped they are stable and not mobile at temperatures at least as high as 700 °C. At 900 °C [Fig. 1(e)], most of the Cr impurities segregate to a narrow surface layer about 0.1 µm thick. We have discussed above that the Cr impurities will be trapped by the defects in the amorphous layer. Our data suggest that Cr–trap complexes, if they have formed for a short time during the annealing, are dissociated at the temperature 900 °C. The Cr atoms emitted from these traps will diffuse to the surface (and part of them are evaporated away from the substrate) to lower the free energy. The XTEM micrograph shows that the implantation damages are only partially healed after 900 °C annealing. There are still traps at EOR range after 900 °C annealing, but the surviving defects are rather large in size compared with the EOR defects at lower annealing temperatures. At 1000 °C [Fig. 1(f)], one can see that even the EOR defects are dissolved and most Cr impurities segregate to the narrow surface layer. Based on the thermal stability argument, it is natural to draw the conclusion that if the Cr and trap concentrations are higher, and thus the precipitates can grow to a larger size, the Cr–trap complexes can survive longer at
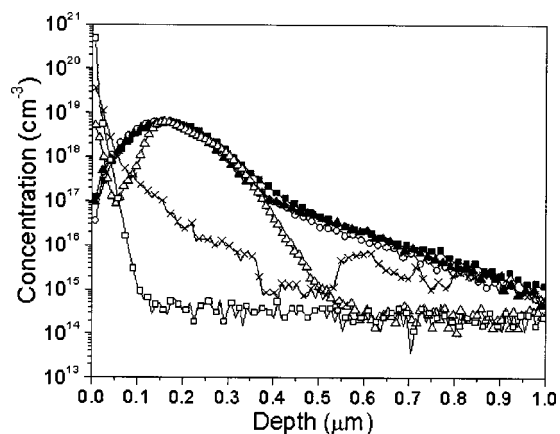
FIG. 3. SIMS depth profiles of ^{52}Cr implanted into silicon substrate at ion energy of 200 keV and a dosage of 1.0×10^{14} ions/cm^2. [■ as implanted, ○ 300 °C, ▲ 500 °C, △ 700 °C, × 900 °C, □ 1000 °C].

the same annealing temperature, for example, 900 °C. This actually has been observed in an earlier work,[21] where the authors show in SIMS profiles that at Cr implantation dosage 1.1×10^{15} ions/cm^2 and ion energy 120 keV, the traps near 70 nm and the EOR defects can survive the 900 °C 30-min annealing. Figure 2 shows SIMS depth profiles for 120 keV, 1.1×10^{15} ions/cm^2 Cr as-implanted and after 900 °C and 1000 °C anneal. The XTEM image annealed at 900 °C is shown scaled appropriately as background. The 900 °C anneal shows Cr removed from the center of the distribution and piled up at the surface. The peaks at 0.07 and 0.19 μm in the SIMS distribution are matched by defects in the XTEM image. The 60 μm diameter SIMS analysis region contains a sufficient number of defects so that the analysis provides the same profile at different spots on the sample. The 1000 °C annealed sample shows Cr remaining only near the surface, similar to the 200 keV, 1.0×10^{15} ions/cm^2 results.

The precipitation behavior of implanted Cr atoms is observed in another set of samples with implantation dosage 1.0×10^{14} ions/cm^2, which is below the amorphization dosage. As we can see from Fig. 3, the Cr distribution begins to shrink at 700 °C. It is obvious that both the surface and the precipitates work as sink for the Cr impurities. The sink near the implantation concentration peak is no longer effective at temperatures above 900 °C, similar to what we have observed in Fig. 1. At 1000 °C, only the surface sink works to achieve solid solubility inside the bulk of silicon.

B. Vanadium implantation

In this part, the diffusion behavior of vanadium in samples with different implantation dosages 1.0×10^{15} ions/cm^2 and 1.0×10^{14} ions/cm^2 will be discussed.

We show in Fig. 4 the SIMS profiles of V atoms in the samples with implantation dosage of 1.0×10^{15} ions/cm^2. The corresponding XTEM micrographs are also shown as the background. A clear amorphous layer is observed in the XTEM image. We cannot observe any appreciable redistribution of V atoms at 300 °C. Similar to what we have observed for the Cr-implanted sample, in Fig. 4(c), after 500 °C
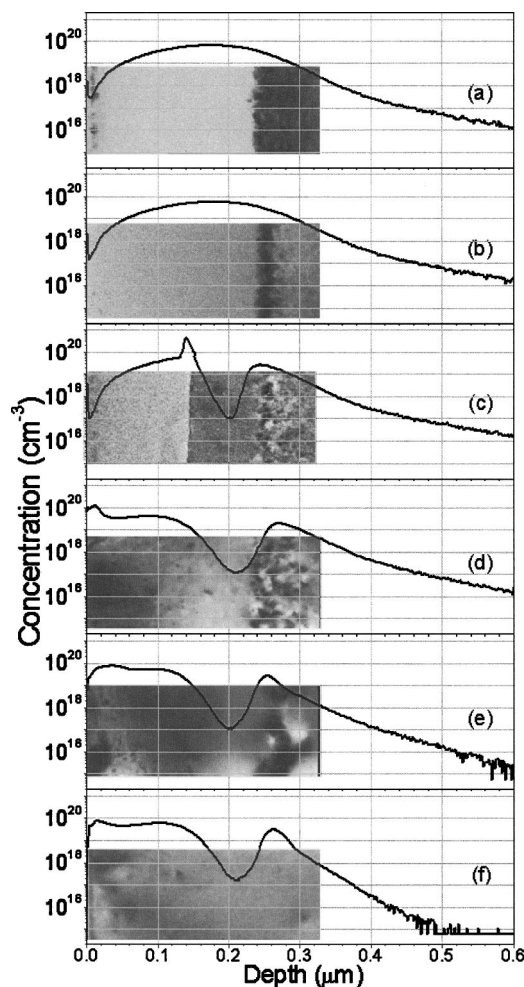

FIG. 4. SIMS depth profiles of ^{51}V implanted into silicon substrate at ion energy of 200 keV and a dosage of 1.0×10^{15} ions/cm^2. (a) as implanted; (b) after 300 °C anneal; (c) after 500 °C anneal; (d) after 700 °C anneal; (e) after 900 °C; and (f) after 1000 °C anneal. The background in each panel is the XTEM micrograph corresponding to the SIMS profile.

annealing we can see clear SPEG together with pileup at the a/c interface. The SPEG velocity is 0.58 Å/s with V implantation dosage of 1.0×10^{15} ions/cm^2. The SPEG velocity is enhanced compared with the intrinsic SPEG velocity and is almost 20% higher than the velocity we observed in the Cr:Si system. This might suggest that the enhancement of SPEG velocity in both Cr- and V-implanted samples is assisted by silicification of metals. As is known, the enthalpy of formation of CrSi$_2$ is about 1.2 eV, while that of VSi$_2$ is 3.2 eV;[36,37] thus, at the same annealing conditions as well as the same V and Cr concentration, the formation of VSi$_2$ is more likely.

After 700 °C annealing, as shown in Fig. 4(d), we observe the plateau concentration similar to that in Fig. 1(d). The explanation is essentially the same as we have discussed. In XTEM images of Figs. 4(d)–(f), we observe precipitates with diameter of about 7 nm in the plateau zone and the area beyond EOR. From the TEM images, it is difficult to determine whether these precipitates are silicon interstitial clusters that trap vanadium atoms. However, they are probably not silicon interstitials because at temperature above 600 °C silicon interstitials will evolve into {311} rod-like de-

fects and at 900 °C, even {311} defects will dissolve and evolve into larger extended defects such as {111} dislocation loops[38] usually accompanied by strong strain field as we have observed from the XTEM image in Fig. 4(e). In fact, from XTEM images we did observe rod-like defects near EOR in samples after 700 °C annealing but not after 900 °C annealing. With annealing temperature of 1000 °C, even the large extended EOR defects are annealed out but these precipitates still survive, as we can observe in Fig. 4(f). From the evolution of these small precipitates under different annealing temperatures, these precipitates are very stable complexes, most probably the chemically bonded VSi_2.

As the density of VSi_2 is 4.62 g/cm^3,[39] one can find approximately 4000 vanadium atoms in one pure VSi_2 precipitate with diameter of 7 nm, which is about the average size of precipitates near 0.16 μm beneath the surface in Fig. 4(e). If we count the number of precipitates near this depth from the XTEM micrograph, measure the average interprecipitate distance of 20 nm, and assume these precipitates are VSi_2, the calculation gives us a bulk density at this depth of about 7×10^{20} cm^{-3}, which is very close to the concentration determined by SIMS. This good agreement between experiments and simple calculation suggests that almost all the vanadium atoms probably exist in the form of VSi_2 precipitates.

Under 900 °C and 1000 °C annealing, less than 10% of the V atoms escape from the silicon substrate. For Cr-implanted samples annealed under the same condition, more than 90% of the Cr atoms leave the substrate. As the atomic masses of ^{52}Cr and ^{51}V are very close, we expect very similar initial damage profiles right after ion implantation. The huge difference between the diffusion and thermal stability of impurity profiles can only be attributed to drastically different impurity-defect interactions. Based on the experiment we have discussed above, the precipitates trapping Cr and V atoms are most probably metal silicide. But, $CrSi_2$ is not as stable as VSi_2 at high temperature (>900 °C) in the bulk of silicon substrate.

As we have shown in Fig. 4, the plateau concentrations are observed in the crystallized silicon layers. We argued that this concentration is related to the accommodation ability of intrinsic defects, which is rather flat in amorphous silicon. If this argument is right for implantation dosage below the amorphization critical dosage ($\sim 2 \times 10^{14}$ $ions/cm^2$ for both Cr and V implantation according to Ref. 14), the area near the ion implantation concentration peak is the most defective area and thus should have the largest accommodation ability for Cr and V atoms. We do observe this in Fig. 3 and in the lower V dosage SIMS profiles shown in Fig. 5. Figure 5 presents the SIMS depth profiles of V atoms in the as-implanted and annealed samples with an implantation dosage of 1.0×10^{14} $ions/cm^2$. There is an obvious shrinkage of the SIMS profiles with increasing annealing temperature. The probable physical procedure is that the larger VSi_2 precipitates are more stable than smaller ones. Thus, during high-temperature annealing, the large ones (initially grown near the implantation concentration peak) are very stable and even grow at the expense of the dissociation of smaller pre-
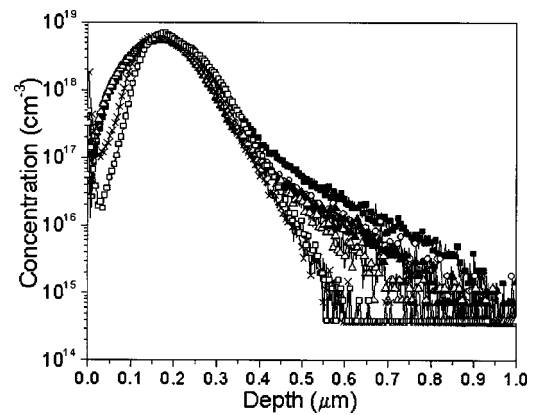

FIG. 5. SIMS depth profiles of ^{51}V implanted into silicon at ion energy of 200 keV and a dosage of 1.0×10^{14} $ions/cm^2$. [■ as implanted, ○ 300 °C, ▲ 500 °C, △ 700 °C, × 900 °C, □ 1000 °C].

cipitates in other areas. Similar contraction due to precipitation is observed in Er-implanted silicon sample with Er peak concentration 3.0×10^{18} cm^{-3} and annealing temperature 1300 °C.[31]

IV. CONCLUSIONS

The combination of SIMS and XTEM analyses of chromium- and vanadium-implanted silicon provide a clearer picture of the diffusion characteristics of these two elements. Implantations above the amorphization dose create defects that are not totally removed by anneals up to 1000 °C. The presence of precipitates and the differences between chromium and vanadium diffusion indicate silicide precipitate formation. Implants below the amorphization dose show somewhat similar results for chromium, but only a narrowing of the distribution for vanadium.

ACKNOWLEDGMENT

[1] K. Graff, *Metal Impurities in Silicon-device Fabrication*, 2nd ed. (Springer, Berlin, 2001).
[2] E. R. Weber, Appl. Phys. A: Solids Surf. **30**, 1 (1983).
[3] A. A. Istratov, H. Hieslmair, and E. R. Weber, Appl. Phys. A: Mater. Sci. Process. **69**, 13 (1999).
[4] A. A. Istratov, H. Hieslmair, and E. R. Weber, Appl. Phys. A: Mater. Sci. Process. **70**, 489 (2000).
[5] N. T. Bendik, V. S. Garnyk, and L. S. Milevski, Sov. Phys. Solid State **12**, 150 (1970).
[6] W. Würker, K. Roy, and J. Hesse, Mater. Res. Bull. **9**, 971 (1974).
[7] J. Zhu, J. Diz, D. Barbier, and A. Laugier, Mater. Sci. Eng., B **4**, 185 (1989).
[8] J. Zhu, G. Chaussemy, and D. Barbier, Appl. Phys. Lett. **54**, 611 (1989).
[9] S. H. Park and D. K. Schroder, J. Appl. Phys. **78**, 801 (1995).
[10] Y. Sato, T. Takahashi, and M. Suezawa, Physica B **308**, 434 (2001).
[11] H. Nakashima, T. Sadoh, H. Kitagawa, and K. Hashimoto, Mater. Sci. Forum **143−147**, 761 (1994).
[12] G. K. Azimov, S. Z. Zainabidinov, and Y. I. Kozlov, Sov. Phys. Semicond. **23**, 1169 (1989).
[13] T. Sadoh and H. Nakashima, Appl. Phys. Lett. **58**, 1653 (1991).
[14] K. S. Jones, S. Prussin, and E. R. Weber, Appl. Phys. A: Solids Surf. **45**, 1 (1988).

[15] J. L. Benton, S. Libertino, P. Kringhoj, D. J. Eaglesham, J. M. Poate, and S. Coffa, J. Appl. Phys. **82**, 120 (1997).

[16] C. Ortiz, D. Mathiot, D. Alquier, C. Dubois, and R. Jerisian, Nucl. Instrum. Methods Phys. Res. B **178**, 188 (2001).

[17] J. X. Xia, T. Saito, R. Kim, T. Aoki, Y. Kamakura, and K. Taniguchi, J. Appl. Phys. **85**, 7597 (1999).

[18] D. Mathiot, A. Claverie, and A. Martinez, Defect Diffus. Forum **153**, 11 (1998).

[19] R. G. Wilson, J. Appl. Phys. **52**, 3954 (1981).

[20] R. G. Wilson, P. K. Vasudev, D. M. Jamba, C. A. Evans, and V. R. Deline, Appl. Phys. Lett. **36**, 215 (1980).

[21] H. Francois-St-Cyr, E. Anoshkina, F. Stevie, L. Chow, K. Richardson, and D. Zhou, J. Vac. Sci. Technol. B **19**, 1769 (2001).

[22] A. Polman, D. C. Jacobson, S. Coffa, J. M. Poate, S. Roorda, and W. C. Sinke, Appl. Phys. Lett. **57**, 1230 (1990).

[23] S. Coffa, J. M. Poate, D. C. Jacobson, W. Frank, and W. Gustin, Phys. Rev. B **45**, 8355 (1992).

[24] A. Y. Kuznetsov and B. G. Svensson, Appl. Phys. Lett. **66**, 2229 (1995).

[25] L. Csepregi, E. F. Kennedy, J. W. Mayer, and T. W. Sigmon, J. Appl. Phys. **49**, 3906 (1978).

[26] G. L. Olson and J. A. Roth, Mater. Sci. Rep. **3**, 1 (1988).

[27] J. A. Roth, G. L. Olson, D. C. Jacobson, and J. M. Poate, Appl. Phys. Lett. **57**, 1340 (1990).

[28] L. Csepregi, E. F. Kennedy, T. J. Gallagher, J. W. Mayer, and T. W. Sigmon, J. Appl. Phys. **48**, 4234 (1977).

[29] S. Coffa, S. Libertino, and C. Spinella, Appl. Phys. Lett. **76**, 321 (2000).

[30] V. E. Borisenko, *Semiconducting Silicides* (Springer, Berlin, New York, 2000).

[31] F. Y. G. Ren, J. Michel, Q. Sun-Paduano, B. Zheng, H. Kitagawa, D. C. Jacobson, J. M. Poate, and L. C. Kimerling, in *Proceedings of the MRS Spring Meeting*, edited by G. S. Pomrenke, P. B. Klein, and D. W. Langer (Materials Research Society, San Francisco, CA, 1993), Vol. 301, p. 87.

[32] D. C. Jacobson, J. M. Poate, and G. L. Olson, Appl. Phys. Lett. **48**, 118 (1986).

[33] S. U. Campisano, E. Rimini, P. Baeri, and G. Foti, Appl. Phys. Lett. **37**, 170 (1980).

[34] A. Y. Kuznetsov, B. G. Svensson, O. Nur, and L. Hultman, J. Appl. Phys. **84**, 6644 (1998).

[35] O. V. Aleksandrov, Y. A. Nikolaev, and N. A. Sobolev, Semiconductors **32**, 1266 (1998).

[36] J. M. Andrews and J. C. Phillips, Phys. Rev. Lett. **35**, 56 (1975).

[37] R. W. Mann and L. A. Clevenger, in *Properties of Metal Silicides*, edited by K. Maex and M. Van Rossum (IEE INSPEC, Stevenage, 1995).

[38] G. Z. Pan and K. N. Tu, J. Appl. Phys. **82**, 601 (1997).

[39] K. Maex, M. Van Rossum, and A. Reader, in *Properties of Metal Silicides*, edited by K. Maex and M. Van Rossum (IEE INSPEC, Stevenage, 1995).